Synthesis, spectroscopic and computational studies of photochromic azobenzene derivatives with 2-azabicycloalkane scaffold

Karolina Kamińska [a,*], Dominika Iwan [a], Alex Iglesias-Reguant [b,c], Weronika Spałek [a], Marek Daszkiewicz [d], Anna Sobolewska [a], Robert Zaleśny [a], Elżbieta Wojaczyńska [a,*], Stanisław Bartkiewicz [a,*]

[a] Faculty of Chemistry, Wroclaw University of Science and Technology, Wybrzeże Wyspiańskiego 27, 50 370 Wrocław, Poland
[b] Faculty of Chemistry, Nicolaus Copernicus University, Gagarina 7, PL-87100 Toruń, Poland
[c] Institut de Química Computacional i Catàlisi (IQCC) and Departament de Química, Universitat de Girona, 17003 Girona, Catalonia, Spain
[d] Institute of Low Temperature and Structure Research, Polish Academy of Sciences, Okólna St. 2, 50-422 Wrocław, Poland

A B S T R A C T

In this study we report the synthesis and photochromic properties of chiral azobenzene derivatives based on the 2-azabicycloalkane skeleton. The photochromic properties of newly synthesized family of azobenzene derivatives have been studied using the UV/Vis spectroscopy. The interpretation of spectral features was supported by the results of the electronic-structure calculations. The experimental data confirm - typical for azobenzene - the occurrence of the *trans–cis* and the *cis–trans* photochemical reactions upon irradiation with the visible and UV light, respectively. On the other side, atypical thermal relaxation processes were observed, especially after UV light irradiation, which indicate that thermal back reaction can be not as straightforward as one could expect. The substituents located on the 2-azabicycloalkane lead to some changes in the electronic structure of studied compounds reflected in the changes of the band shapes in the electronic spectra.

1. Introduction

Azobenzene and its derivatives are well-known photochromic compounds capable of reversible isomerization between the *trans* and the *cis* isomers upon exposure to UV or visible light, or due to thermal stimulus. Azobenzenes, known for over a century, are still frequently investigated for their use in the fundamental and applied research [1]. Susceptibility to light-induced transformations places azobenzene-based compounds in privileged spot as they are used in optical processing and data storage, holography, optical switching and fabrication of optical elements [2–10]. Moreover, there are numerous possible applications of various assemblies containing the azobenzene unit as the photoswitchable molecules exhibiting various activities in biological systems [11]: *(i)* they show potential for protein modulation as the *cis–trans* isomerization of a linker connecting two parts of the polypeptide chain can result in significant conformational changes [12]; *(ii)* the ability to control the enzymatic activity of a histone deacetylase-like amidohydrolase with an azobenzene switch with a long-lived *cis* form was demonstrated as well [13]; *(iii)* rationally designed azobenzene-based photoswitches were applied for the efficient two-photon neuronal excitation [14]; *(iv)* light-controlled chloride binding was applied for the construction of *trans*-membrane transporters of these ions [15]; *(v)* driving and photo-regulation of myosin-actin motors at molecular and macroscopic levels could be performed by photo-responsive high energy molecules [16]; and *(vi)* photoswitchable kinesin inhibitor enabled a reversible chromosome movement and progression of mitose [17]. The huge potential of the azobenzene-based compounds as light-activated ingredients of biological systems encouraged us to synthesize a series of derivatives bearing 2-azabicycloalkane scaffold shown in Schemes 1–3. The aim of this study is to report on the photochromism of this newly synthesized family of compounds. More specifically, we seek to confirm the occurrence and efficiency of photochemical reactions for all members of the series. To that end we will apply experimental spectroscopic methods and electronic-structure calculations.

2. Materials and methods

2.1. Materials for synthesis

Reagents and solvents were purchased from the chemical companies (additional purification was not performed). Melting point was determined by Schmelzpunkt Bestimmer Apotec melting point

* Corresponding authors.
E-mail addresses: karolina.kaminska@pwr.edu.pl (K. Kamińska), elzbieta.wojaczynska@pwr.edu.pl (E. Wojaczyńska), stanislaw.bartkiewicz@pwr.edu.pl (S. Bartkiewicz).

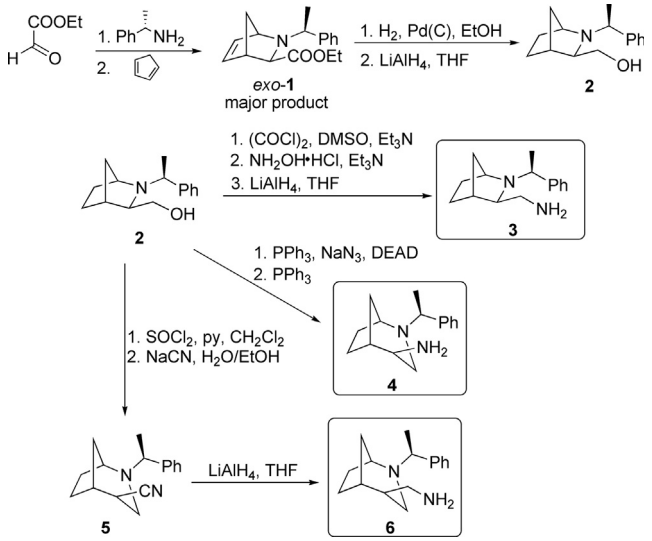

Scheme 1. The multi-step synthesis of chiral 2-azabicyclic substrates **3**–**4** and **6** for further azobenzene derivatives synthesis.

apparatus (WEPA Apothekenbedarf GmbH & Co. KG., Hillscheid, Germany) in a standard open capillary. ^{1}H and ^{13}C NMR spectra were measured with Jeol 400yh (Jeol Ltd., Tokyo, Japan). Chloroform-d was used as a solvent. Chemical shifts and coupling constants are expressed using standard units, ppm and Hz respectively. Waters LCT Premier XE TOF spectrometer (Waters Corporation, Milford, MA, USA) was utilized for high-resolution mass spectra measurement using the electrospray ionization mode. The automatic polarimeter model AA-5 (Optical Activity, Ltd., Ramsey, UK) was used to determine the optical rotation ($[\alpha]_D^{20}$ values are expressed in 10^{-1} deg cm^2 g^{-1}). Infrared spectra were recorded in a 4000–400 cm^{-1} range using Perkin Elmer 2000 FTIR instrument (PerkinElmer, Waltham, MA, USA). The column chromatography and thin-layer chromatography were performed using silica gel 60 (60–200 μm, 70–230 mesh) as absorbent.

2.2. Preparation of starting compounds

Synthesis and modifications of *aza*-Diels-Alder adduct **1** were conducted as reported in previous papers [17–20].

2.3. Preparation of amines **3, 4** and **6**

Amines (1*S*,3*R*,4*R*)-2-[(*S*)-1-phenylethyl]-3-aminemethyl-2-azabicyclo[2.2.1]heptane **3**, (1*S*,4*S*,5*R*)-2-[(*S*)-1-phenylethyl]-4-amine-2-azabicyclo(3.2.1)octane **4** and (1*S*,4*S*,5*R*)-4-chloro-2-[(*S*)-1-phenylethyl]-2-azabicyclo(3.2.1)octane **6** were synthesized according to the procedures developed and described previously by our group [19–21].

2.4. Preparation of sulfonamide**s 8** and **9**

Amine **3** or **4** (230 mg, 1.0 mmol) was dissolved in 15 mL of dichloromethane.

4-(dimethylamino)azobenzene-4′-sulfonyl chloride **7** (324 mg, 1.0 mmol) and powdered potassium hydroxide (100 mg, 1.8 mmol) were added. The mixture was stirred at room temperature for 24 h. The reaction was worked up by addition of water and extraction with dichloromethane (3x10 ml). Combined organic phases were dried over anhydrous sodium sulfate, filtered and the solvent was evaporated under the vacuum. The residue was chromatographed on the silica with mixture of *n*-hexane- ethyl acetate 1:1 (v/v) as an eluent, to give pure compounds **8** and **9** in high yield (450 mg, 87% and 361 mg, 70%, respectively). Copies of ^{1}H and ^{13}C NMR spectra are available in Supplementary Material.

2.4.1. 4-((*E*)-(4-(dimethylamino)phenyl)diazenyl)-*N*-(((1*S*,3*R*,4*R*)-2-((*S*)-1-phenylethyl)-2-azabicyclo[2.2.1]heptan-3-yl)methyl) benzenesulfonamide (**8**)

Orange solid. Yield 450 mg (87%), mp. 194–196 ℃, $[\alpha]_D^{20}$ = +123.3 (c 0.69, CH_2Cl_2).

^{1}H NMR (400 MHz, $CDCl_3$): δ 1.19–1.42 (m, 7H), 1.55–1.63 (m, 1H), 1.80–1.93 (m, 3H), 2.02–2.04 (m, 1H), 2.14–2.21 (m, 2H), 3.12 (s, 6H), 3.38 (q, *J* = 6.4 Hz, 1H), 3.58 (s, 1H), 6.76–6.80 (m, 2H), 7.03–7.07 (m, 3H), 7.15–7.18 (m, 2H), 7.62–7.64 (m, 2H), 7.83–7.86 (m, 2H), 7.92–7.94 (m, 2H) ppm. ^{13}C NMR (100 MHz, $CDCl_3$): δ 22.3, 22.5, 29.5, 35.7, 40.1, 41.9, 47.1, 58.8, 60.9, 67.6, 111.6, 122.5, 125.8, 127.5, 127.6, 127.9, 128.4, 139.1. 143.7, 145.7, 153.1, 155.4 ppm. IR (KBr): 824, 1092, 1136, 1164, 1364, 1516, 1602, 1735, 2871, 2936, 2971, 3271, 3437 cm^{-1}. HRMS (ESI$^+$, *m*/*z*): calcd for $C_{29}H_{35}N_5O_2S$ ($[M + H]^+$) 518.2590; found 518.2585.

2.4.2. 4-((*E*)-(4-(dimethylamino)phenyl)diazenyl)-*N*-((1*S*,4*S*,5*R*)-2-(1-phenylethyl)-2-azabicyclo[3.2.1]octan-4-yl)benzenesulfonamide (**9**)

Pale-orange solid. Yield 361 mg (70%), mp. 168–170 ℃, $[\alpha]_D^{20}$ = +19.8 (*c* 0.20, CH_2Cl_2).

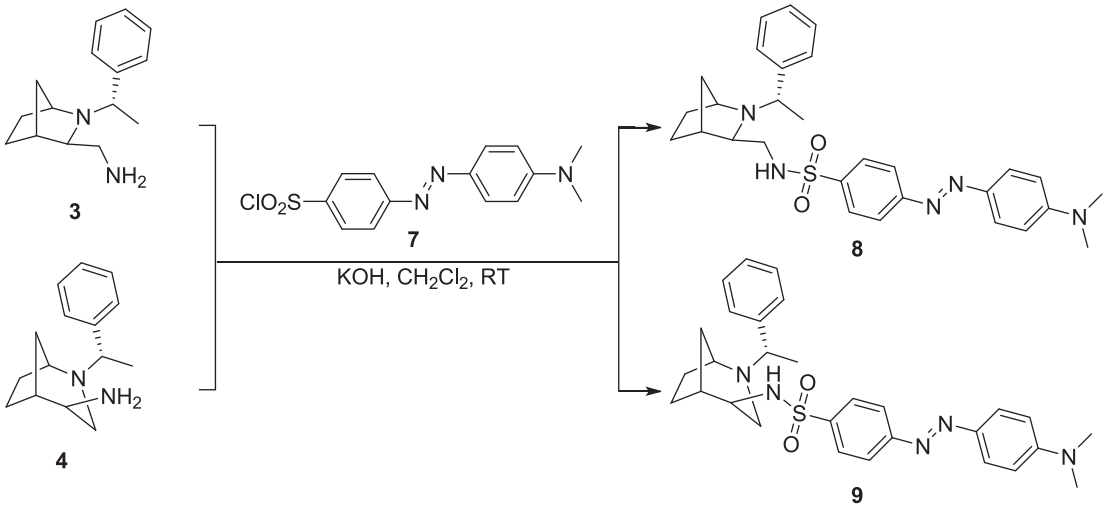

Scheme 2. The synthesis of the azobenzene sulfonamides **8** and **9.**

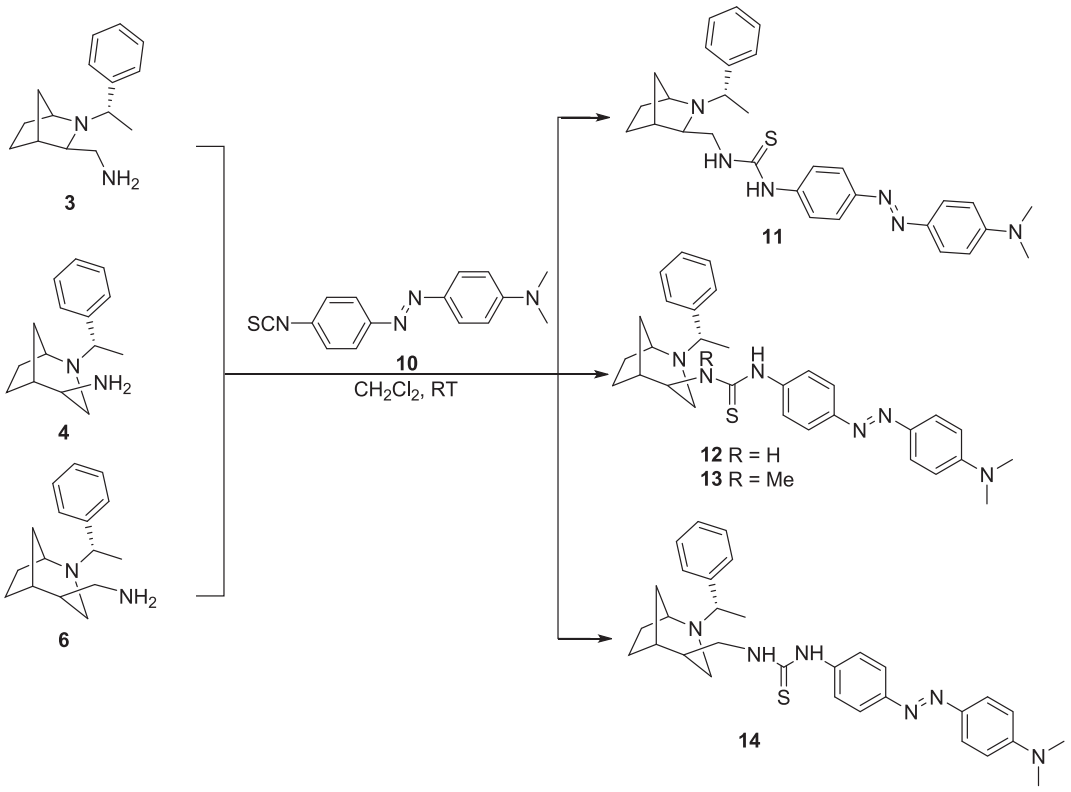

Scheme 3. The synthesis of the azobenzene thioureas **11**–**14**.

^{1}H NMR (400 MHz, $CDCl_3$): δ 1.24–1.28 (m, 7H), 1.62–1.68 (m, 3H), 1.84–1.90 (m, 1H), 2.06–2.09 (m, 1H), 2.28 (m, 1H), 3.04–3.20 (m, 7H), 3.52 (m, 1H), 5.09 (br s, 1H), 6.76–6.80 (m, 2H), 7.14–7.16 (m, 2H), 7.21–7.25 (m, 3H), 7.71 (m, 4H), 7.90–7.92 (m, 2H) ppm. ^{13}C NMR (100 MHz, $CDCl_3$): δ 21.1, 21.8, 27.2, 34.4, 39.9, 40.4, 49.1, 52.7, 55.8, 62.3, 111.6, 122.6, 125.7, 127.2, 127.7, 128.6, 140.3, 143.7, 144.9, 153.1, 155.2 ppm. IR (KBr): 821, 1140, 1167, 1336, 1366, 1421, 1520, 1603, 2821, 2947, 3435 cm^{-1}. HRMS (ESI$^+$, *m*/*z*): calcd for $C_{29}H_{35}N_5O_2S$ ([M + H]$^+$) 518.2590; found 518.2596.

2.5. Preparation of thioureas ***11 – 14***

Amine **3** or **6** (1.0 mmol) was dissolved in 15 mL of dichloromethane and commercially available 4-(4-isothiocyanatophenylazo)-*N*, *N*-dimethylaniline **10** (1.0 mmol) was added. The mixture was stirred at room temperature for 24 h. The reaction was worked up by addition of water and extraction with dichloromethane (3x10 ml). Combined organic phases were dried over anhydrous sodium sulfate, filtered and the solvent was evaporated under the vacuum. The residue was chromatographed on the silica with mixture of dichloromethane and methanol 95:5 (*v*/*v*) as an eluent, to give pure compounds **11** and **14** in high yield (480 mg, 93% and 274 mg, 52%, respectively).

Reaction between amine **4** (1.0 mmol) and 4-(4-isothiocyanatophenylazo)-*N*,*N*-dimethylaniline **10** (1.0 mmol) led to a mixture of thiourea **12** and a side-product thiourea **13**. Both products were isolated using column chromatography (*n*-hexane-ethyl acetate 1:1 (v/v) on the silica), characterized and tested in our studies (280 mg, 54% and 79 mg, 15%, respectively). Copies of ^{1}H and ^{13}C NMR spectra are available in Supplementary Material.

*2.5.1. 1-(4-((E)-(4-(dimethylamino)phenyl)diazenyl)phenyl)-3-(((1S,3R,4R)-2-[(S)-1-phenylethyl]-2-azabicyclo[2.2.1]heptan-3-yl) methyl)thiourea (**11**)*

Pale-orange solid. Yield 480 mg (93%), mp. 190–192 ℃, $[\alpha]_D^{20}$ = +10.1 (*c* 0.57, CH_2Cl_2).

^{1}H NMR (400 MHz, $CDCl_3$): δ 1.18–2.57 (m, 13H), 3.09 (s, 1H), 3.26–3.81 (m, 2H), 6.49 (br s, 1H), 6.71–6.78 (m, 2H), 7.05–7.35 (m, 6H), 7.53–7.67 (m, 1H), 7.88–7.95 (m, 4H), 11.96 (br s, 1H) ppm. ; ^{13}C NMR (150 MHz, $CDCl_3$): δ 14.2, 22.2, 29.6, 35.9, 40.3, 43.4, 48.9, 58.48, 60.6, 61.4, 66.8, 68.9,111.5, 122.9, 123.8, 124.9, 125.2, 127.5, 127.7, 128.2, 128.4, 128.7, 136.9,140.8, 143.0, 143.5, 143.6, 143.8, 145.2, 151.6, 152.7, 179.0 ppm. IR (KBr): 703, 1139, 1151, 1279, 1365, 1517, 1600, 2871, 2968, 3214, 3436 cm^{-1}. HRMS (ESI$^+$, *m*/*z*): calcd for $C_{30}H_{36}N_6S$ ([M + H]$^+$) 513.2800; found 513.2807.

*2.5.2. 1-(4-((E)-(4-(dimethylamino)phenyl)diazenyl)phenyl)-3-((1S,4S,5R)-2-((S)-1-phenylethyl)-2-azabicyclo[3.2.1]octan-4-yl) thiourea (**12**)*

Orange solid. Yield 280 mg (54%), mp. 170–172 ℃, $[\alpha]_D^{20}$ = +251.0 (*c* 0.48, CH_2Cl_2). ^{1}H NMR (400 MHz, $CDCl_3$): δ 1.20–1.47 (m, 5H), 1.59 (s, 3H), 1.71–1.76 (m, 2H), 2.22–2.41 (AB, 2H), 2.72–2.75 (m, 1H), 3.11 (s, 6H), 3.25 (q, *J* = 6.4 Hz, 1H), 3.51 (m, 1H), 4.12 (br s, 1H), 6.78 (d, *J* = 9.2 Hz, 3H), 7.03–7.04 (m, 2H), 7.16–7.20 (m, 3H), 7.30 (d, *J* = 8.4 Hz, 1H), 7.58 (br s, 1H), 7.96 (dd, J_1 = 8.8 Hz, J_2 = 36 Hz, 4H) ppm. ^{13}C NMR (100 MHz, $CDCl_3$): δ 21.0, 22.0, 27.2, 35.3, 37.5, 40.4, 49.4, 54.5, 55.9, 62.2, 111.6, 124.1, 125.2, 125.3, 127.0, 128.5, 136.6, 143.6, 145.4, 151.7, 152.8, 178.4 ppm. IR (KBr): 801, 1025, 1097, 1138, 1154, 1262, 1312, 1324, 1364, 1526, 1602, 2963, 3270, 3436 cm^{-1}. HRMS (ESI$^+$, *m*/*z*): calcd for $C_{30}H_{36}N_6S$ ([M + H]$^+$) 513.2800; found 513.2791.

*2.5.3. 3-(4-((E)-(4-(dimethylamino)phenyl)diazenyl)phenyl)-1-methyl-1-((1S,4S,5R)-2-((S)-1-phenylethyl)-2-azabicyclo[3.2.1]octan-4-yl)thiourea (**13**)*

Orange solid. Yield 79 mg (15%), mp. 150–152 ℃, $[\alpha]_D^{20}$ = +9.8 (*c* 0.96, CH_2Cl_2). ^{1}H NMR (400 MHz, $CDCl_3$): δ 1.32–1.50 (m, 7H), 1.71–1.91 (m, 3H), 2.18–2.21 (m, 1H), 2.39–2.62 (AB, 2H), 2.73 (br s, 1H), 3.08 (s, 6H), 3.39 (q, *J* = 6.4 Hz, 1H), 3.50 (s, 3H), 3.88–3.91 (m, 1H), 6.77 (d, *J* = 9.2 Hz, 2H), 6.97–6.98 (m, 2H), 7.12–7.20 (m, 3H), 7.48 (d, *J* = 8.4 Hz, 2H), 7.87–7.91 (m, 4H) ppm. ^{13}C NMR (100 MHz, $CDCl_3$): δ 1.1, 20.6, 21.7, 27.0, 27.7, 33.5, 38.6, 40.4, 46.7, 56.5, 62.5, 63.9, 111.6, 122.6, 124.9, 126.9, 127.6, 127.8, 128.6, 142.1, 143.8, 150.5, 152.4, 180.6 ppm. IR (KBr) 701, 947, 1136, 1155, 1245, 1366, 1527, 1600, 1736, 2865, 2948, 3156, 3324, 3382 cm^{-1}. HRMS (ESI$^+$, *m*/*z*): calcd for $C_{31}H_{38}N_6S$ ([M + H]$^+$) 527.2879; found 527.2626.

*2.5.4. 1-(4-((E)-(4-(dimethylamino)phenyl)diazenyl)phenyl)-3-(((1S,4R,5R)-2-((S)-1-phenylethyl)-2-azabicyclo[3.2.1]octan-4-yl)methyl)thiourea (**14**)*

Orange solid. Yield 274 mg (52%), mp. 125–127 ℃, $[\alpha]_D^{20}$ = +162.6 (*c* 0.02, CH_2Cl_2). ^{1}H NMR (400 MHz, $CDCl_3$): δ 1.28–1.67 (m, 11*H*), 2.30 (m, 2H), 2.60 (s, 2H), 3.09 (s, 6H), 3.42–3.89 (m, 3H), 6.77 (d, *J* = 6.8 Hz, 2H), 7.33–7.52 (m, 8H), 7.83 (dd, J_1 = 8.8 Hz, J_2 = 27.2 Hz, 4H). ^{13}C NMR (100 MHz, $CDCl_3$): δ 14.1, 22.7, 23.5, 29.4, 29.7, 30.4, 31.9, 35.6, 40.3, 41.0, 70.6, 111.6, 111.9, 123.2, 123.3, 124.0, 125.0, 128.4, 129.2, 143.7, 152.4, 181.2 ppm. IR (KBr) 701, 947, 1136, 1155, 1245, 1366, 1527, 1600, 1736, 2865, 2948, 3156, 3324, 3382 cm^{-1}. HRMS (ESI$^+$, *m*/*z*): calcd for $C_{31}H_{38}N_6S$ ([M + H]$^+$) 527.2957; found 527.2955. Additionally, X-ray measurement was performed for **14** to confirm its structure (see Supplementary Material).

2.6. Photochromic properties

The investigations were performed using a Shimadzu UV-2101PC spectrophotometer which was modified by building-in two LEDs. One of the diodes emits UV light at the wavelength 372 nm while the other emits visible light at 465 nm. Such configuration allows to illuminate the sample without removing it from the spectrometer holder, thus daylight has no effect on measurements. The cuvette holder was equipped with the magnetic stirrer and modified in such a way to allow illumination of the sample through an aperture perpendicular to the spectrophotometer beam. The samples of studied compounds were dissolved in chloroform ($\sim 10^{-6}$–10^{-4} M) and placed in the quartz cuvette (1 cm optical path, 3 cm^3 volume). Thanks to introduced modifications, enabling simultaneous irradiating and stirring, the entire solution of the sample was homogenously illuminated. Measurements were carried out at ambient temperature (295 K).

2.7. Computational methods

Geometries of the *cis* and *trans* isomers of **8**–**9** and **11**–**14** in chloroform solution were optimized based on the density functional theory with the aid of the M06-2X exchange–correlation functional [22] and the 6-31G** basis set. Solvent effects were taken into account by means of the IEF-PCM model [23]. Minima on the potential energy hypersurface were confirmed by the evaluation of hessian. The vertical excitation energies were computed using the PBE0 exchange–correlation functional [24–25] and the 6-311++G** basis set. We have also performed electronic-structure calculations using range-separated CAM-B3LYP functional and highly-parametrized member of Minnesota functionals (MN15). The results are shown in Table S3-S5 and demonstrate that PBE0 delivers the most accurate spectral signatures for studied compounds. All electronic-structure calculations have been performed using the GAUSSIAN 16 program [26].

3. Results and discussion

3.1. Synthesis

In our study we synthesized the optically pure azobenzene derivatives with 2-azabicycloalkane scaffold and sulfonamide and thiourea functionalities. The base compound, necessary to obtain the investigated derivatives, was an alcohol **2** with 2-azanorbornane backbone, prepared by the stereoselective *aza*-Diels-Alder reaction between cyclopentadiene and *in situ* generated chiral Schiff base, a subsequent double bond hydrogenation, and ester moiety reduction [18–21,27–31]. Further transformation of an alcohol **3** allows for the preparation of bicyclic amines **3**, **4** and **6** which play a crucial role in the final products synthesis (Scheme 1). Based on the nucleophilic substitution reaction between a chiral bicyclic substrate **3**, **4**, **6** and a commercially available azobenzene derivatives **7** and **10** (in the presence of base for sulfonamides **8** and **9**), it was possible to obtain the target products with high chemical yield (52–93%) (Schemes 2–3). Interestingly, the nucleophilic substitution of **4** with isothiocyanate **10** led to the main product **12** (54%) and its *N*-methylated adduct **13** in 15% yield (Scheme 3) [32]. The newly obtained derivatives were fully characterized and subsequently used in photochromic studies.

3.2. Photochromic properties

Photochromic properties of the compounds **8**–**9** and **11**–**14** dissolved in chloroform were investigated using the UV–Vis spectroscopy [33–39]. Photochromic behavior was studied by using two wavelengths, namely 372 nm and 465 nm (see Section 2.6 for details), in two separate experiments. In the first experiment, before any irradiation, the absorption spectrum of the sample was measured (the spectrum of so called the initial state). Subsequently, the sample was irradiated for 1 min with visible light (10 mW/cm^2) in order to induce photochemical reaction. The next spectrum of the sample was recorded right after the light source was turned off. The subsequent spectra were measured at different times, counted from the moment when the light was turned off, and they reflect thermal relaxation process. The second experiment was conducted likewise, however UV light (10 mW/cm^2) was used instead to induce the photochemical reaction. Both experiments were performed using the same sample solution. The irradiation by UV light was performed the day after the experiment with visible light. The sample was kept in the dark between the experiments. As a result of that some differences in the initial spectra before visible and UV light irradiation can be noticed.

Fig. 1 gathers the results of studies on photochemical reactions in the synthesized **8**–**9** and **11**–**14** compounds. Graphs on the left side (Fig. 1) demonstrate the changes in the absorption spectrum due to the *trans*–*cis* isomerization induced by the visible light and due to the following thermal relaxation process. Graphs on the right side of the figure show the changes in the spectrum resulting from the *cis*–*trans* reaction induced by irradiation with the UV light and thermal back reaction. Each graph in Fig. 1 shows the absorption spectrum of the compound solution before the irradiation and the change in the spectrum due to photochemical reaction induced by 1 min of irradiation either by the visible (Fig. 1.1a)–1.6a)) or UV light (Fig. 1.1b)–1.6b)), and the changes in the absorption spectrum resulting from thermal isomerization.

The relative efficiency of the photochemical reaction, the reaction efficiency RE_{LIGHT}(where *LIGHT* stands for VIS or UV irradiation), has been defined and calculated according to the equation:

$$RE_{LIGHT} = \frac{|A_0 - A_{LIGHT}|}{A_{iso}} \quad (1)$$

where A_0 is the value of the absorbance at the wavelength that corresponds to the maximum of the band before irradiation, A_{LIGHT} is the absorbance after 1 min of the irradiation either by the visible or UV light measured for the same wavelength as before irradiation, and A_{iso} is the absorbance at the wavelength corresponding to the position of the isosbestic point that is localized the closest to the maximum of the absorption band. It is worth to emphasize that the relative reaction efficiency defined by Eq. (1) is independent on concentration (in the wide range). The results are gathered in Table 1.

Fig. 1 reveals photochromic properties of newly synthesized family of azobenzene derivatives bearing 2-azabicycloalkane scaffold. Photochemical reactions induced either by the visible (the *trans–cis* isomerization) or UV (the *cis–trans* isomerization) light effectively occur in compounds and once the light is turned off the effective thermal back isomerization is observed. The efficiency of reactions differs depending on which wavelength was used for irradiation. For all studied compounds the reaction induced by the visible light occurred more effectively in comparison to the reaction induced by UV light (RE_{VIS} is significant larger

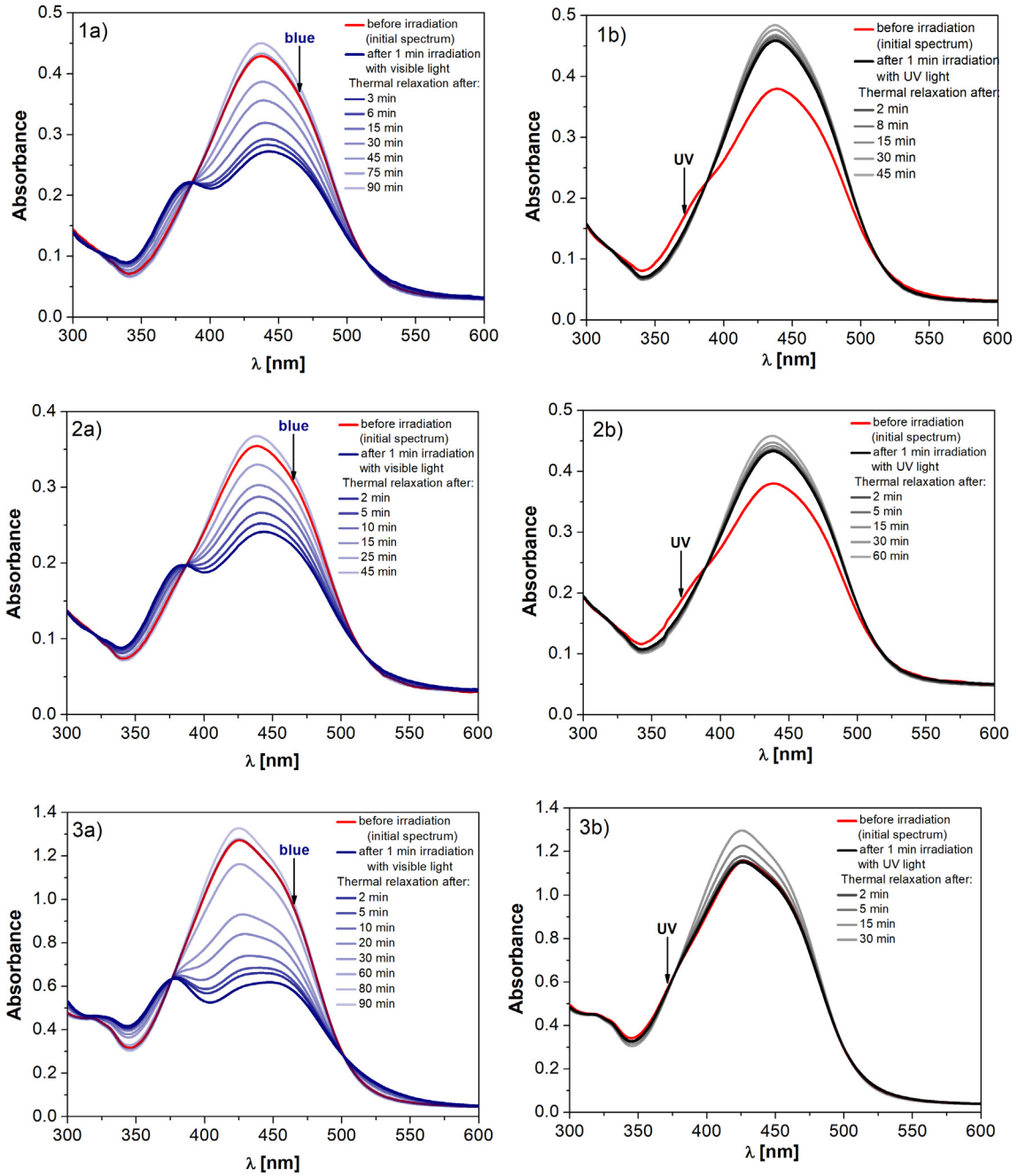

Fig. 1. Changes in the absorption spectra resulting from the *trans–cis* (1a-6a) graphs) and the *cis–trans* (1b-6b) graphs) photochemical reactions and due to the following thermal back reaction for all studied compounds: (1) **8**, (2) **9**, (3) **11**, (4) **12**, (5) **13** and (6) **14**. The absorption spectrum of the compound before (red line) and after irradiation with a) visible light (λ_{Vis} = 460 nm) (the darkest blue line) and b) UV light (λ_{UV} = 372 nm) (the black line). Spectra measured at different times after the light was switched off (marked by different shades of blue and black color) demonstrate the changes in the spectrum resulted from thermally driven isomerization. Arrows indicate wavelengths of light used for induction of photochemical reactions. (For interpretation of the references to color in this figure legend, the reader is referred to the web version of this article.)

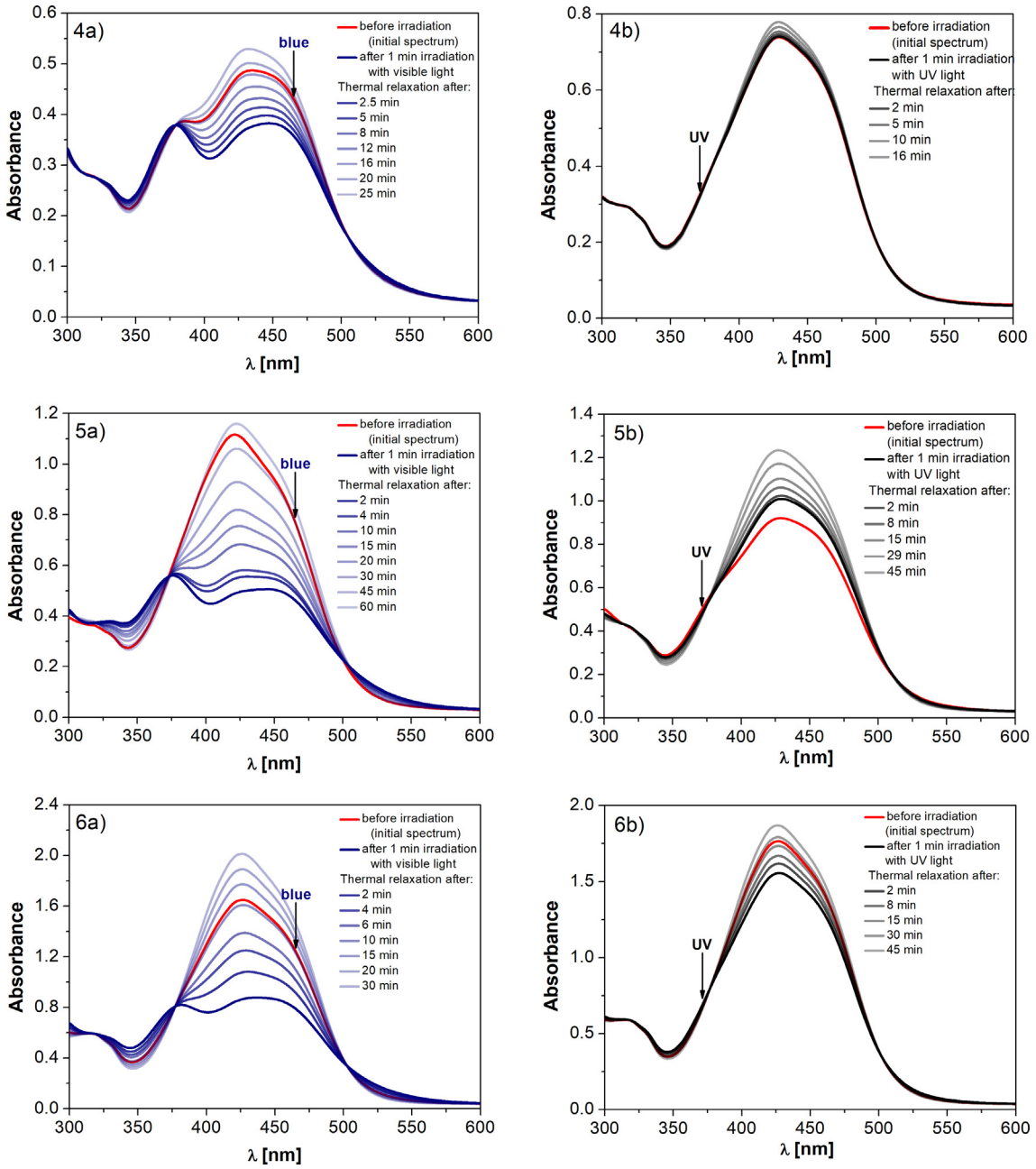

Fig. 1 (*continued*)

Table 1
The relative reaction efficiency of photochemical reactions induced either by visible (RE_{VIS}) or UV (RE_{UV}) light.

Compound	**8**	**9**	**11**	**12**	**13**	**14**
RE_{VIS}	0.72	0.58	1.07	0.29	1.12	0.97
RE_{UV}	0.34	0.22	0.01	0.02	0.17	0.26

than RE_{UV}, cf. Table 1). Among all studied compounds, the most effective *trans–cis* isomerization with comparable efficiency was measured for compounds **11**, **13** and **14** which are thioureas. Some differences in the chemical structure of these compounds (the 6-membered 2-azanorbornane unit (**11**), the 7-membered bridged azepane framework with the substituted NH group of the thiourea moiety (**13**), the thiourea moiety moved away from the bridged azepane system (**14**)) have no clear influence on the efficiency of the reaction. Lower efficiency of the reaction, nevertheless meaningful, was observed for compounds **8** and **9** which belong to the group of sulfonamide derivatives (slightly higher efficiency was measured for the compound with a bicyclic 2-azanorbornane system (**8**)). The lowest efficiency was observed for **12**. The *cis–trans* isomerization occurred with significantly lower efficiency in comparison to the *trans–cis* one. The effective reaction induced by UV light was observed for compounds **8**, **9**, **13** and **14**, while for compounds **11** and **12** the efficiency was very low.

Table 2
Summary of the electronic-structure calculations for compounds **8**–**9** and **11**–**14** using the PBE0 exchange–correlation functional. Wavelengths (λ) correspond to three the lowest-energy vertical electronic excitations of the *trans* and the *cis* isomers of **8**–**9** and **11**–**14**. The values of oscillator strengths (f, dimensionless) are given in parentheses.

Compound	$S_0 \rightarrow S_1$		$S_0 \rightarrow S_2$		$S_0 \rightarrow S_3$	
	cis λ [nm] (f)	*trans* λ [nm] (f)	*cis* λ [nm] (f)	*trans* λ [nm] (f)	*cis* λ [nm] (f)	*trans* λ [nm] (f)
8	466 (0.1379)	460 (0.0010)	370 (0.0020)	437 (1.2464)	364 (0.2286)	414 (0.0007)
9	476 (0.2156)	461 (0.0002)	369 (0.2789)	439 (1.1950)	369 (0.0031)	410 (0.0270)
11	477 (0.1679)	444 (0.0017)	359 (0.2618)	431 (1.3776)	343 (0.0287)	366 (0.0099)
12	477 (0.1664)	444 (0.0257)	359 (0.2524)	432 (1.3843)	347 (0.0326)	369 (0.0094)
13	483 (0.1945)	444 (0.0023)	358 (0.2530)	431 (1.3792)	351 (0.0460)	375 (0.0157)
14	484 (0.1979)	444 (0.0017)	358 (0.2730)	431 (1.3776)	343 (0.0107)	366 (0.0099)

Further detailed analysis of the experimental absorption spectra will be supported by theoretical studies.

In order to unravel spectral features shown in Fig. 1, the electronic structures of the *trans* and the *cis* isomers of the compounds **8**–**9** and **11**–**14** were determined based on quantum chemical calculations.

Table 2 contains summary of these calculations for three lowest-energy electronic excitations (see also corresponding Fig. S21 in the SI file). There are several interesting conclusions that can be drawn from these results. The main intense absorption band in experimental spectra with maxima in the range 421–439 nm can be assigned to the $S_0 \rightarrow S_2$ electronic transition for the *trans* isomer. The $S_0 \rightarrow S_1$ electronic excitation in the *trans* isomer has negligible oscillator strengths, except the compound **12**. The long-wavelength shoulders close to 450 nm in the absorption band in the spectrum before irradiation for this compound is due to the $S_0 \rightarrow S_1$ electronic excitation. Moreover, the electronic $S_0 \rightarrow S_1$ transition for the *cis* isomer is found to be red-shifted with respect to its counterpart for the *trans* isomer. The corresponding wavelength for the *cis* isomer is to a large extent system-dependent and one finds its variations close to 20 nm on passing from **8** to **14**; nevertheless in the case of all compounds the $S_0 \rightarrow S_1$ electronic excitation for the *cis* isomer share a common feature – it is characterized by a significant value of the oscillator strength. These results, taken together, allow to explain the changes in experimental absorption spectra on passing from **8** to **14**. Namely, the spectra

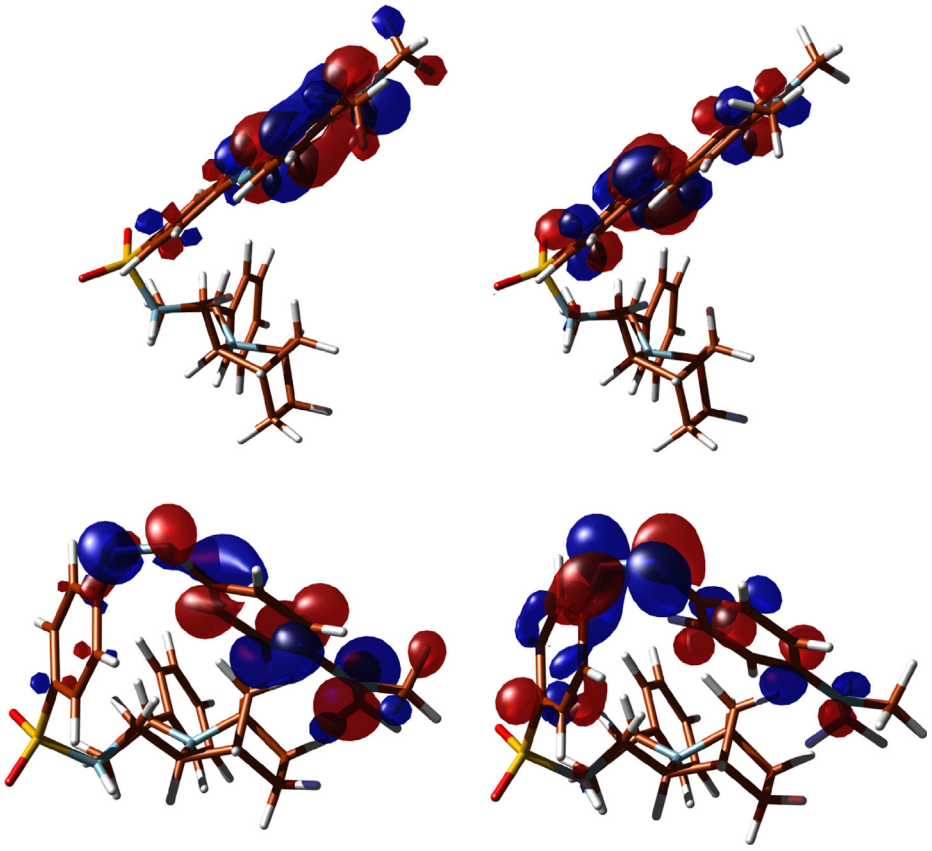

Fig. 2. Frontier molecular orbitals (HOMO: left, LUMO: right) for the *trans* (top) and the *cis* (bottom) isomers of the compound **8**.

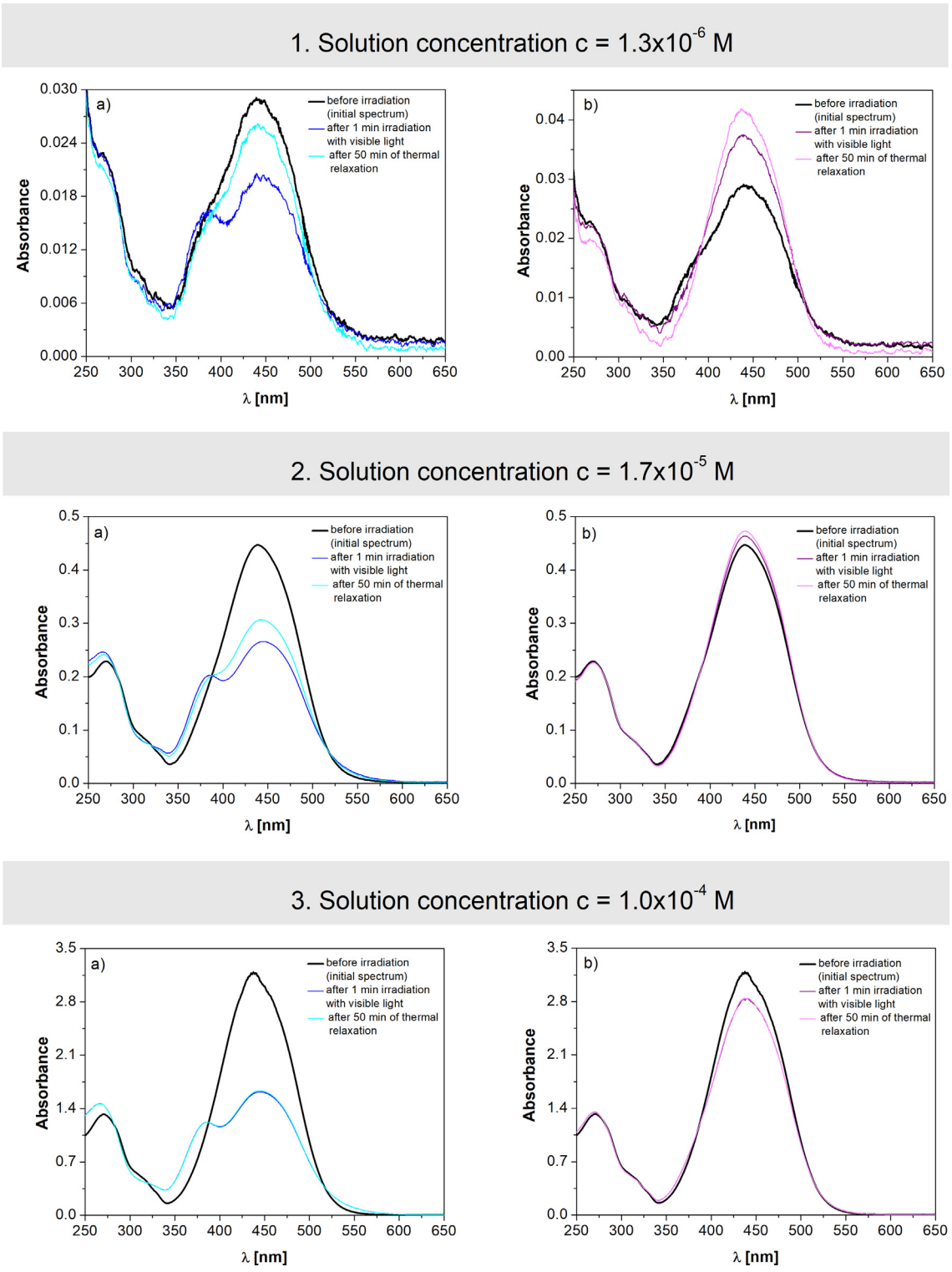

Fig. 3. Changes in the absorption spectrum of the compound **8** solution in chloroform before and after irradiation with visible light (on the left: 1a), 2a) and 3a)) and UV light (on the right: 1b), 2b) and 3b)) for different solution concentrations. Changes in the absorbance due to thermally driven isomerization - spectrum measured 50 min after the light was switched off.

of **8** (or **9**) (sulfonamide derivatives) after irradiation shows structureless broad absorption band with maxima at 439 nm which is a composition of neighbouring electronic transitions $S_0 \rightarrow S_2$ (large intensity; the *trans* isomer) and $S_0 \rightarrow S_1$ (small intensity; the *cis* isomer). For compounds **11**–**14** (thiourea derivatives) one finds that the main band in the absorption spectra is more structured than that observed for **8** and **9**. For instance, the spectra of **11** shows a band with the maximum at 426 nm and a shoulder at 450 nm, indicating overlapping bands corresponding to at least two electronic states (see Table 2). Upon irradiation of the compound **11** the relative intensity of the feature at 450 nm increases in comparison to the feature at 426 nm. The same holds for compounds **12**–**14**. However, in the case of the compound **14**, as revealed by electronic-structure calculations, these two electronic transitions

are distinctly separated which results in the well-structured wide absorption band showing two distinct maxima.

As demonstrated by the analysis of the electronic structure, both the $S_0 \rightarrow S_2$ transition (the *trans* isomer) and the $S_0 \rightarrow S_1$ transition (the *cis* isomer) are dominated by one-electron HOMO → LUMO orbital transitions. These frontier orbitals for both isomers of **8** are shown in Fig. 2. The electronic density difference plots for both isomers of all compounds (see Figures S22-S33 in the SI file) demonstrate that in the case of the brightest transition ($S_0 \rightarrow S_2$) the corresponding density changes are localized on the azobenzene moiety. This holds for both isomers. One can thus conclude that the azabicycloalkane scaffold is not involved in intramolecular charge-transfer transitions to the lowest $\pi\pi^*$ excited states.

With the help of results from electronic-structure calculations, we will now start the analysis of experimental spectra discussing the results for the compound **8** as a representative of whole series. As it can be seen on Figure 1.1 the absorption spectrum of the non-irradiated sample (the initial state) is characterized by a single strong absorption band localized at λ_{max} = 438 nm which, as demonstrated by the electronic-structure calculations, corresponds to the $S_0 \rightarrow S_2$ electronic transition of the *trans*-isomer. Irradiation of the solution with visible light induces the *trans–cis* reaction which leads to the photostationary state dominated by the *cis* isomer. As a result, the intensity of the band was reduced and it was bathochromically shifted from λ_{max} = 438 nm to $\lambda_{max,1}$ = 442 nm, while in the range of shorter wavelength a new absorption band was built up at wavelength $\lambda_{max,2}$ = 384 nm (cf. Fig. 1.1a)). The new band is related to the *cis* isomer and its concentration in solution increases after irradiation. The assignment of this band is supported by the results of the electronic-structure calculations. The spectrum after irradiation shows the broad absorption band which is a composition of neighbouring electronic transitions $S_0 \rightarrow S_2$ (large intensity; the *trans* isomer) and $S_0 \rightarrow S_1$ (small intensity; the *cis* isomer). After the light is switched off thermal *cis–trans* back reaction takes place, i.e. the spectrum returns towards the initial state. Fig. 1.1a) shows that after ca. 75 min the spectrum returned to its initial shape and intensity (before illumination). Moreover, a further monitoring of the relaxation process resulted in obtaining the spectrum with increased intensity of the band maximum in comparison to the initial one, which is a striking result (Fig. 1.1a)). It is worth to point out, that the increase of the intensity of the band maximum above the value of the initial state was observed for all studied compounds (cf. Fig. 1.2a) – 1.6a)). The significant changes in the absorption spectra and the preserved positions of the isosbestic points, observed in Fig. 1.1a)–1.6a), confirm the occurrence of photochemical reaction induced by visible light.

Illumination of the studied compound **8** with UV light, which causes the *cis–trans* isomerization, resulted in an increase of the intensity of the absorption band maximum, as one can notice in Fig. 1.1b). The direction of the change of the spectrum is opposite to the one observed when visible light was used. It is in accordance with the mechanism of isomerization of the azobenzene core and it is understandable since wavelengths corresponding to the UV and the visible light range are located on the opposite sides of the isosbestic point. After the light is switched off and when the thermal back reaction begins it could be expected that the intensity of the main band in the spectrum will decrease as the result of the return of the system to its thermodynamic equilibrium (the decrease of concentration of the *cis* form). Unexpectedly, the behavior of the absorption spectra measured during the relaxation process shows something opposite – the intensity of the band maximum, despite the lack of light, was further increasing (cf. Fig. 1.1b)). The increase of the intensity of the band maximum during thermal back isomerization was observed for the other studied compounds as well (see Fig. 1.2b)–1.6b)). The results demonstrate that the thermal back reaction is a complex process in studied azobenzene derivatives. We will conclude the analysis of the spectroscopic data highlighting that the results demonstrate that photochemical reaction induced by UV light is observed and this holds for all studied compounds.

Both striking observations related to the thermal back reaction, i.e., *(i)* further increase of the intensity of the band after switching off the UV light, and *(ii)* an increase of the intensity of the band above the intensity of the initial state after switching off visible light, suggest the preference of the compound to achieve the equilibrium state by forming the larger amount of the *trans* isomers. In order to shed light on this interesting photochromic phenomenon, further additional experiments were carried out for **8**. Three solutions with a different concentration, namely 1.3×10^{-6}, 1.7×10^{-5} and 1.0×10^{-4} M were prepared. The samples were subsequently irradiated with the visible and UV light for 1 min. The initial spectrum, the change in the spectrum resulted from irradiation and the spectrum after 50 min after switching off the light were measured. The results have been gathered in Fig. 3.

The strongest and significant increase of the intensity of the band above the intensity of the initial spectrum after UV irradiation and further increase of the intensity due to thermal relaxation was observed for the solution of the lowest concentration (Fig. 3.1b)). For the solution of the intermediate concentration the effect was still observed, however was less pronounced (Fig. 3.2b)). For the solution with the highest concentration (two orders of magnitude larger than the lowest concentration) UV caused a decrease of the intensity of the band and no changes of the spectrum were observed due to thermal relaxation (Fig. 3.3b)). The concentration had no influence on the direction of spectrum changes due to visible light irradiation (cf. Fig. 3.1a), 3.2a) and 3.3a)). In this case a decrease of the band was observed regardless of the concentration of the solution. The concentration affected the efficiency of the *trans–cis* isomerization. The strongest change in the absorbance due to visible irradiation was observed for the solution of the largest concentration. In that case the increase of the intensity of the band above the intensity of the initial spectrum due to thermal relaxation was not observed. These results clearly demonstrate that concentration is one of the factors which determine the direction of the photochemical reaction in the studied azobenzene derivative.

Additional experiment using the ^{1}H NMR technique was performed to confirm the stability of **8** and monitoring thermal relaxation processes after UV/Vis light exposure. No changes in the structure of the studied compound after UV/Vis irradiation were observed. The NMR study could not shed light on which species are present after irradiation due to very low sample concentration. The mechanism behind the observed relaxation processes after irradiation in the studied compounds seems complicated. Presumably, it may be related to the mixture of several conformers arising from the presence of 2-azabicycloalkne-containing moiety. The presence of the fixed isosbestic points excludes the hypothesis of unusual photochromic behavior due to $(trans)_n \rightarrow n(trans)$ processes. Despite of the lack of full understanding of the mechanism, that could explain observations made during relaxation processes at this stage of the research, it is clear, based on reported results, that effective photochemical reactions occur in the azobenzene derivatives with 2-azabicycloalkane moiety. Taking into account the effective *trans––cis-trans* isomerization of the azobenzene core and the presence of the chiral substituent (2-azabicycloalkane fragment), we plan to perform the studies of light-controlled biological activity of the investigated compounds which will be reported elsewhere.

4. Conclusions

The photochromic properties of newly synthesized azobenzene derivatives containing 2-azabicycloalkane scaffold have been stud-

ied using the UV/Vis spectroscopy and further supported by the computational quantum-chemistry methods. The experimental data confirm typical for azobenzene the *trans–cis* and the *cis–trans* photochemical reactions upon irradiation with the visible and UV light, respectively. However, the analysis of the spectra due to the thermal back reaction for the samples illuminated by the UV radiation shows the preference of the studied compounds to achieve the equilibrium state by forming the larger amount of the *trans* isomer (the band maximum further increased after exposure to the UV radiation). Furthermore, we demonstrated that the concentration is one of the factors which affects the thermal relaxation processes. In the case of some of the derivatives the spectra after irradiation show well-structured shape which, as revealed by electronic-structure calculations, arises from overlapping bands from the *trans* and the *cis* isomers. Taken together, the results presented in this work have revealed that the mechanism underlying the relaxation processes is rather complex, however, most importantly, they have proved that effective photochemical reactions occur for all studied azobenzene derivatives. It opens the possibility of using of these newly synthesized compounds in studies of light-controlled biological activity.

CRediT authorship contribution statement

Karolina Kamińska: Conceptualization, Investigation, Data curation, Writing – original draft. **Dominika Iwan:** Investigation, Writing – original draft. **Alex Iglesias-Reguant:** Investigation, Data curation, Visualization. **Weronika Spałek:** Investigation. **Marek Daszkiewicz:** Investigation, Visualization. **Anna Sobolewska:** Visualization, Writing – review & editing. **Robert Zaleśny:** Supervision, Data curation, Writing – review & editing. **Elżbieta Wojaczyńska:** Conceptualization, Supervision, Writing – review & editing. **Stanisław Bartkiewicz:** Conceptualization, Supervision, Writing – review & editing.

Data availability

Data will be made available on request.

Declaration of Competing Interest

The authors declare that they have no known competing financial interests or personal relationships that could have appeared to influence the work reported in this paper.

Acknowledgements

This work was financially supported by the National Science Center (NCN) Poland [grant number DEC-2018/29/B/ST3/00829]. Authors thank Wroclaw Centre for Networking and Supercomputing for computational resources and ILT&SR PAS for financial support by statutory activity subsidy.

Appendix A. Supplementary material

Supplementary data to this article can be found online at https://doi.org/10.1016/j.molliq.2022.119869.

References

[1] F.A. Jerca, V.V. Jerca, R. Hoogenboom, Advances and opportunities in the exciting world of azobenzenes, Nat. Rev. Chem. 6 (1) (2022) 51–69, https://doi.org/10.1038/s41570-021-00334-w.
[2] R. Hagen, T. Bieringer, Photoaddressable polymers for optical data storage, Adv. Mater. 13 (2001) 1805–1810, https://doi.org/10.1002/1521-4095(200112)13:23<1805::AID-ADMA1805>3.0.CO;2-V.
[3] S. Hvilsted, C. Sanchez, R. Alcala, The volume holographic optical storage potential in azobenzene containing polymers, J. Mater. Chem. 19 (2009) 6641–6648, https://doi.org/10.1039/B900930M.
[4] A. Sobolewska, S. Bartkiewicz, J. Myśliwiec, K.D. Singer, Holographic memory devices based on a single-component phototropic liquid crystal, J. Mater. Chem. C 2 (2014) 1409–1412, https://doi.org/10.1039/C3TC32361G.
[5] N.K. Viswanathan, D.Y. Kim, S. Bian, J. Williams, W. Liu, L. Li, L. Samuelson, J. Kumar, S.K. Tripathy, Surface relief structures on azo polymer films, J. Mater. Chem. 9 (1999) 1941–1955, https://doi.org/10.1039/A902424G.
[6] A. Natansohn, P. Rochon, Photoinduced motions in azo-containing polymers, Chem. Rev. 102 (2002) 4139–4175, https://doi.org/10.1021/cr970155y.
[7] K.G. Yager, C.J. Barrett, Novel photo-switching using azobenzene functional materials, J. Photochem. Photobiol. A: Chem. 182 (2006) 250–261, https://doi.org/10.1016/j.jphotochem.2006.04.021.
[8] S.M. Gan, A.R. Yuvaraj, M.R. Lutfor, M.Y. Mashitah, H. Gurumurthy, Synthesis, liquid crystal characterization and photo-switching studies on fluorine substituted azobenzene based esters, RSC Adv. 5 (2015) 6279–6285, https://doi.org/10.1039/C4RA13700K.
[9] E. Madiahlagan, Z. Ngaini, G. Hegde, Synthesis, liquid crystalline properties and photo switching properties of coumarin-azo bearing aliphatic chains: Application in optical storage devices, J. Mol. Liq. 292 (2019) 111328, https://doi.org/10.1016/j.molliq.2019.111328.
[10] M. Alaasar, S. Poppe, Hockey-Stick Polycatenars: Network formation and transition from one dimensional to three-dimensional liquid crystalline phases, J. Mol. Liquids 351 (2022) 118613, https://doi.org/10.1016/j.molliq.2022.118613.
[11] A. Beharry, G.A. Woolley, Azobenzene photoswitches for biomolecules, Chem. Soc. Rev. 40 (2011) 4422–4443, https://doi.org/10.1039/C1CS15023E.
[12] M. Zhu, H. Zhou, Azobenzene-based small molecular photoswitches for protein modulation, Org. Biomol. Chem. 16 (2018) 8434–8445, https://doi.org/10.1039/C8OB02157K.
[13] M. Korbus, G. Balasubramanian, F. Müller-Plathe, H. Kolmar, F.J. Meyer-Almes, Azobenzene switch with a long-lived cis-state to photocontrol the enzyme activity of a histone deacetylase-like amidohydrolase, Biol. Chem. 395 (2013) 401–412, https://doi.org/10.1515/hsz-2013-0246.
[14] L.S. Weiss, M.O. Borgh, A. Blinova, T. Ollikainen, M. Möttönen, J. Ruostekoski, D.S. Hall, Controlled creation of a singular spinor vortex by circumventing the Dirac belt trick, Nat. Commun. 10 (1) (2019), https://doi.org/10.1038/s41467-019-12787-1.
[15] Y.R. Choi, G.C. Kim, H.G. Jeon, J. Park, W. Namkung, K.S. Jeong, Azobenzene-based chloride transporters with light-controllable activities, Chem. Commun. 50 (2014) 15305–15308, https://doi.org/10.1039/C4CC07560A.
[16] H.M. Menezes, M.J. Islam, M. Takahashi, N. Tamaoki, Driving and photoregulation of myosin–actin motors at molecular and macroscopic levels by photo-responsive high energy molecules, Org. Biomol. Chem. 15 (2017) 8894–8903, https://doi.org/10.1039/c7ob01293d.
[17] N.N. Mafy, K. Matsuo, S. Hiruma, R. Uehara, N. Tamaoki, Photoswitchable CENP-E inhibitor enabling the dynamic control of chromosome movement and mitotic progression, J. Am. Chem. Soc. 142 (2020) 1763–1767, https://doi.org/10.1021/jacs.9b12782.
[18] E. Wojaczyńska, J. Wojaczyński, K. Kleniewska, M. Dorsz, T.K. Olszewski, 2-Azanorbornane—A versatile chiral aza-Diels–Alder cycloadduct: Preparation, applications in stereoselective synthesis and biological activity, Org. Biomol. Chem. 13 (2015) 6116–6148, https://doi.org/10.1039/C5OB00173K.
[19] D. Iwan, K. Kamińska, E. Wojaczyńska, M. Psurski, J. Wietrzyk, M. Daszkiewicz, Biaryl sulfonamides based on the 2-azabicycloalkane skeleton—synthesis and antiproliferative activity, Materials 13 (2020) 5010, https://doi.org/10.3390/ma13215010.
[20] E. Wojaczyńska, I. Turowska-Tyrk, J. Skarżewski, Novel chiral bridged azepanes: Stereoselective ring expansion of 2-azanorbornan-3-yl methanols, Tetrahedron 68 (2012) 7848–7854, https://doi.org/10.1016/j.tet.2012.07.028.
[21] K. Kamińska, E. Wojaczyńska, J. Wietrzyk, E. Turlej, A. Błażejczyk, R. Wieczorek, Synthesis, structure and antiproliferative activity of chiral polyamines based on a 2-azanorbornane skeleton, Tetrahedron Asymmetry 27 (2016) 753–758, https://doi.org/10.1016/j.tetasy.2016.06.009.
[22] Y. Zhao, D.G. Truhlar, The M06 suite of density functionals for main group thermochemistry, thermochemical kinetics, noncovalent interactions, excited states, and transition elements: two new functionals and systematic testing of four M06-class functionals and 12 other functionals, Theoretical Chem. Accounts 120 (2008) 215–241, https://doi.org/10.1007/s00214-007-0310-x.
[23] J. Tomasi, B. Mennucci, E. Cances, The IEF version of the PCM solvation method: an overview of a new method addressed to study molecular solutes at the QM ab initio level, J. Mol. Struct. (Theochem) 464 (1999) 211–226, https://doi.org/10.1016/S0166-1280(98)00553-3.
[24] C. Adamo, V. Barone, Toward reliable density functional methods without adjustable parameters: The PBE0 model, J. Chem. Phys. 110 (13) (1999) 6158–6170, https://doi.org/10.1063/1.478522.
[25] M. Ernzerhof, G.E. Scuseria, Assessment of the Perdew–Burke–Ernzerhof exchange-correlation functional, J. Chem. Phys. 110 (11) (1999) 5029–5036, https://doi.org/10.1063/1.478401.
[26] M. J. Frisch, G. W. Trucks, H. B. Schlegel, G. E. Scuseria, M. A. Robb, J. R. Cheeseman, G. Scalmani, V. Barone, B. Mennucci, G. A. Petersson, H. Nakatsuji, M. Caricato, X. Li, H. P. Hratchian, A. F. Izmaylov, J. Bloino, G. Zheng, J. L. Sonnenberg, M. Hada, M. Ehara, K. Toyota, R. Fukuda, J. Hasegawa, M. Ishida, T. Nakajima, Y. Honda, O. Kitao, H. Nakai, T. Vreven, J. A. Montgomery Jr, J. E. Peralta, F. Ogliaro, M. Bearpark,J. J. Heyd, E. Brothers, K. N. Kudin, V. N. Staroverov, R. Kobayashi, J. Normand, K. Raghavachari, A. Rendell, J. C. Burant, S. S. Iyengar, J. Tomasi, M. Cossi, N. Rega, J. M. Millam, M. Klene, J. E. Knox, J. B. Cross, V. Bakken, C. Adamo, J. Jaramillo, R. Gomperts, R. E. Stratmann, O. Yazyev, A. J. Austin, R. Cammi, C. Pomelli, J. W. Ochterski, R. L. Martin, K.

Morokuma, V. G. Zakrzewski, G. A. Voth, P. Salvador, J. J. Dannenberg, S. Dapprich, A. D. Daniels, Ö. Farkas, J. B. Foresman, J. V. Ortiz, J. Cioslowski, D. J. Fox, Gaussian 2009. Gaussian Inc. Wallingford CT (2009).

[27] P.D. Bailey, R.D. Wilson, G.R. Brown, Stereoselective synthesis of pipecolic acid derivatives using aza-Diels-Alder reactions, Tetrahedron Lett. 30 (1989) 6781–6784, https://doi.org/10.1016/S0040-4039(00)70675-7.

[28] L. Stella, H. Abraham, J. Feneau-Dupont, B. Tinant, J.P. Declercq, Asymmetric aza-Diels-Alder reaction using the chiral 1-phenyl ethyl imine of methyl glyoxylate, Tetrahedron Lett. 31 (18) (1990) 2603–2606, https://doi.org/10.1016/0040-4039(90)80136-A.

[29] H. Waldmann, M. Braun, Asymmetric synthesis of bicyclic amino acid derivatives by *aza*-Diels-Alder reactions in aqueous solution, Liebigs. Ann. Chem. (1991) 1045–1048, https://doi.org/10.1002/jlac.1991199101180.

[30] H. Nakano, N. Kumagai, C. Kabuto, H. Matsuzaki, H. Hongo, Synthesis of new chiral catalysts, N-alkyl-2-azanorbornyl-methanols, for the enantioselective addition of diethylzinc to arylaldehydes, Tetrahedron: Asymmetry 6 (1995) 1233–1236, https://doi.org/10.1016/0957-4166(95)00151-E.

[31] J.K. Ekegren, S.A. Modin, D.A. Alonso, P.G. Andersson, Multigram scale synthesis of a useful *aza*-Diels–Alder adduct in a one-step procedure, Tetrahedron: Asymmetry 13 (2002) 447–449, https://doi.org/10.1016/S0957-4166(02)00127-1.

[32] J.E. Mills, C.A. Maryanoff, D.F. McComsey, R.C. Stanzione, L. Scott, Reaction of amines with methylene chloride. Evidence for rapid aminal formation from N-methylenepyrrolidinium chloride and pyrrolidine, J. Org. Chem. 52 (1987) 1857–11185, https://doi.org/10.1021/jo00385a038.

[33] H. Orlikowska, A. Sobolewska, S. Bartkiewicz, Light-responsive surfactants: Photochromic properties of water-soluble azobenzene derivatives, J. Mol. Liq. 316 (2010), https://doi.org/10.1016/j.molliq.2020.113842 113842.

[34] A. Miniewicz, H. Orlikowska, A. Sobolewska, S. Bartkiewicz, Kinetics of thermal *cis–trans* isomerization in a phototropic azobenzene-based single-component liquid crystal in its nematic and isotropic phases, Phys. Chem. Chem. Phys. 20 (2018) 2904–2913, https://doi.org/10.1039/C7CP06820D.

[35] J. García-Amorós, D. Velasco, Recent advances towards azobenzene-based light driven real-time information-transmitting materials, Beilstein J. Org. Chem. 8 (2012) 1003–1017, https://doi.org/10.3762/bjoc.8.113.

[36] Z. Lin, S. Wang, Q. Yan, Q. Yan, D. Cao, Visible light/Cu^{2+} dual triggered photochromic donor-acceptor stenhouse adducts: Synthesis, properties and applications, Dyes Pigm. 191 (2021), https://doi.org/10.1016/j.dyepig.2021.109384 109384.

[37] Q. Yan, C. Li, S. Wang, Z. Lin, Q. Yan, D. Cao, Visible light responsive donor-acceptor stenhouse adducts with indoline-tri/tetra-phenylethylene chromophore: Synthesis, aggregation-induced emission, photochromism and solvent dependence effect, Dyes Pigm. 178 (2020), https://doi.org/10.1016/j.dyepig.2020.108352 108352.

[38] L. Ma, C. Li, Q. Yan, S. Wang, W. Miao, D. Cao, Unsymmetrical photochromic bithienylethene-bridge tetraphenylethene molecular switches: Synthesis, aggregation-induced emission and information storage, Chin. Chem. Lett 32 (2020) 361–364, https://doi.org/10.1016/j.cclet.2019.07.040.

[39] M.L. Rahman, G. Hegde, M. Azazpour, M.M. Yusoff, S. Kumar, Synthesis and characterization of liquid crystalline azobenzene chromophores with fluorobenzene terminal, J. Fluor. Chem. 156 (2013) 230–235, https://doi.org/10.1016/j.jfluchem.2013.10.004.